Journal of Physics G: Nuclear and Particle Physics

PAPER • OPEN ACCESS

Precision mass measurements of cesium isotopes—new entries in the ISOLTRAP chronicles

To cite this article: D Atanasov *et al* 2017 *J. Phys. G: Nucl. Part. Phys.* **44** 044004

OPEN ACCESS
IOP Publishing

Made open access 12 September 2017
Journal of Physics G: Nuclear and Particle Physics

J. Phys. G: Nucl. Part. Phys. **44** (2017) 044004 (10pp) https://doi.org/10.1088/1361-6471/aa5a20

Precision mass measurements of cesium isotopes—new entries in the ISOLTRAP chronicles

D Atanasov[1], D Beck[2], K Blaum[1], Ch Borgmann[1], R B Cakirli[3], T Eronen[1,9], S George[1], F Herfurth[2], A Herlert[4], M Kowalska[5], S Kreim[5], Yu A Litvinov[3], D Lunney[6], V Manea[5,6], D Neidherr[2], M Rosenbusch[7,10], L Schweikhard[7], F Wienholtz[5,7], R N Wolf[7,11] and K Zuber[8]

[1] Max-Planck-Institut für Kernphysik, D-69117 Heidelberg, Germany
[2] GSI Helmholtzzentrum für Schwerionenforschung, D-64291 Darmstadt, Germany
[3] Department of Physics, Istanbul University, 34134 Istanbul, Turkey
[4] FAIR GmbH, D-64291 Darmstadt, Germany
[5] CERN, 1211 Geneva, Switzerland
[6] CSNSM-IN2P3-CNRS, Université Paris-Sud, F-91406 Orsay, France
[7] Ernst-Moritz-Arndt-Universität, Institut für Physik, D-17487 Greifswald, Germany
[8] Technische Universität Dresden, D-01069 Dresden, Germany

E-mail: dinko.atanasov@cern.ch

Received 16 November 2016, revised 13 January 2017
Accepted for publication 18 January 2017
Published 23 February 2017

Abstract

Alkali ion beams are among the most intense produced by the ISOLDE facility. These were the first to be studied by the ISOLTRAP mass spectrometer and ever since, new measurements have been regularly reported. Recently the masses of very neutron-rich and short-lived cesium isotopes were determined at ISOLTRAP. The isotope ^{148}Cs was measured directly for the first time by Penning-trap mass spectrometry. Using the new results, the trend of two-neutron separation energies in the cesium isotopic chain is revealed to be smooth and gradually decreasing, similar to the ones of the barium and xenon isotopic chains. Predictions of selected microscopic models are employed for a discussion of the experimental data in the region.

[9] Present Address: University of Jyväskylä, PO Box 35 (YFL), FI-40014, Finland.
[10] Present Address: RIKEN Nishina Center, 2-1 Hirosawa, Wako-shi, Saitama 351-0198, Japan.
[11] Present Address: ARC Centre of Excellence for Engineered Quantum Systems, School of Physics, The University of Sydney, NSW 2006, Australia.

Keywords: penning trap mass spectrometer ISOLTRAP, ISOLDE/CERN, atomic masses of cesium isotopes

(Some figures may appear in colour only in the online journal)

1. Introduction

The radioactive ion-beam facility ISOLDE/CERN [1] has proven to be an excellent place for performing precision mass measurements of short-lived isotopes, most recent examples of which can be found in [2–7]. The two most important characteristics of the laboratory are the high intensities of delivered radioactive ion-beams and the good beam emittance allowing for efficient and controlled injection into sensitive apparatus. The history of the facility highlights a number of key mass measurements carried out in the late seventies and throughout the eighties at the Orsay's double-focusing mass spectrometer [8, 9], which demonstrated the importance of direct mass measurements of short-lived nuclides.

Following the success of these measurements, in the mid eighties the Penning-trap mass spectrometer ISOLTRAP was installed at ISOLDE [10]. This project was motivated by the increased demand for more precise atomic masses of short-lived nuclides [11]. It is important to emphasize that this necessity is still present today, which one can illustrate by the number of Penning-trap projects operating (or under commissioning) at radioactive ion-beam facilities (see table 2 in [12]). The Penning-trap mass spectrometry is to date the most powerful tool allowing to reach the highest control over precision and accuracy in atomic mass measurements.

The atomic mass is a gross property reflecting the sum effect from all the interplaying forces in the nucleus [13]. More specifically, studying new atomic masses in long chains of nuclides, where varying only a single parameter, e.g. the neutron number, enables one to study fine nuclear structure effects. Hence, examining carefully the mass surface that is composed by the whole ensemble of nuclides including those far away from stability one can follow the evolution of nuclear structure. To unveil the nuclear effects, such as shell and sub-shell closures, the onset of deformation and the pairing effects, the masses of short-lived nuclides need to be measured with uncertainties of 10–100 keV/c^2. Currently, this level of precision is better than the most accurate mass models allowing for the stringent test of their predictive power [14]. Moreover, it provides a reliable data for nucleosynthesis model calculations [15–17].

Isotopes of alkali elements, such as rubidium and cesium [18–21] were the first elements studied by the ISOLTRAP collaboration. Over the years these isotopic chains were covered by many Penning-trap measurements revealing interesting nuclear structure phenomena far away from stability. In the rubidium isotopic chain, the most exotic isotope measured so far is the short-lived ^{100}Rb reaching into the region of deformed nuclei starting at $N = 60$ [5]. Here we reports on new data resulting from the same experimental campaign. Initially, mass measurements of neutron-rich copper isotopes had been scheduled, but those had to be canceled due to unexpected difficulties with the target unit. However, the target provided enough surface ionized beams for an alternative program.

The contents of the paper, discusses the latest layout of the ISOLTRAP mass spectrometer and is structured as follows: first an introduction to the experimental setup is given, then highlights of the measurement principle and the new results are presented, and finally, the data are compared to the predictions of several microscopic models.

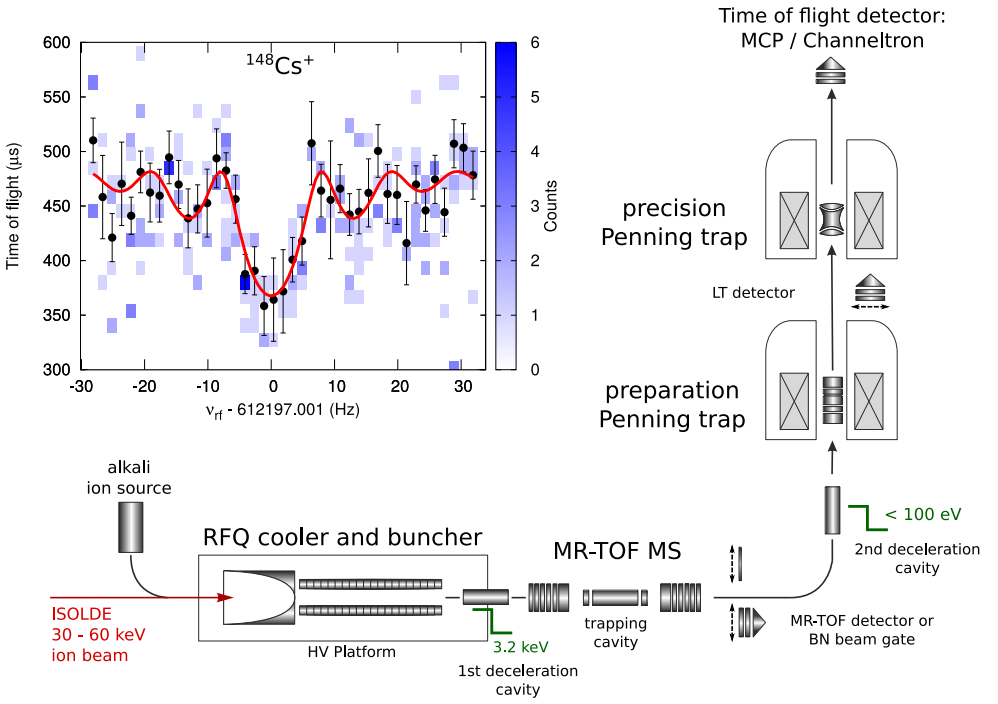

Figure 1. Schematic drawing of the mass spectrometer ISOLTRAP. The main components of the setup are indicated, as well as detectors used for monitoring ion transfer and for measuring the time-of-flight resonances. The inset presents a time-of-flight ion-cyclotron resonance spectrum of the ^{148}Cs isotope, in which the flight time of the ejected ions to the detector is plotted as a function of the quadrupolar excitation frequency in the precision Penning trap. The number of counts in each frequency step is given by the color code. The solid line represents the fit of the theoretical curve to the data points.

2. Experimental setup

The cesium isotopes of interest were produced by using a pulsed proton beam with an energy of 1.4 GeV impinged on a UCx target [1]. The so produced radioactive atoms were extracted from the target container by thermal diffusion, followed by surface ionization. The target temperature was varied between 1800 °C and 2000 °C during the experimental run in order to optimize the extraction efficiency for neutron-rich cesium. Singly charged ions were created in the ion-source. They were then accelerated to 50 keV and sent through the ISOLDE's high resolution separator for first-stage removal of unwanted contaminations.

Today, the ISOLTRAP setup consists of a segmented linear radio-frequency quadrupole trap (RFQ) [22] a multi-reflection time-of-flight mass separator (MR-TOF MS) [23, 24], a preparation as well as a precision Penning traps, the latter two devices are placed in the center of superconducting magnets [25, 26]. The main components of the full setup are sketched in figure 1.

The beam from ISOLDE is accumulated, cooled down by collisions with a helium buffer-gas, and bunched in the RFQ trap at the entrance of ISOLTRAP. After an accumulation time of some 10 ms in the RFQ, the ion bunch is extracted. Prior to the injection into the MR-TOF MS its energy is adapted to the beam-line potential by a pulsed drift cavity [27]. Afterwards,

the ions are captured into the MR-TOF MS. Once trapped, they perform multiple oscillations between two electrostatic mirrors. With every oscillation the overall flight path increases and therefore the separation power of the device to resolve isobars. In the described experiment, the MR-TOF MS was used in combination with a Bradbury–Nielsen beam gate [28] working as a fast ion selector and allowing a resolving power on the order of 10^5 for a separation time of a few tens of milliseconds. Purified ion pulses were then delivered to the first Penning trap. In this cylindrical trap a mass-selective technique was applied, in which the ions of interest were centered by using a quadrupolar RF excitation in combination with buffer-gas cooling [29]. Afterwards, the cooled and isobarically pure ion bunch was transferred to the hyperbolically shaped precision Penning trap for the actual mass measurement.

3. Principle of mass measurements

The mass m_{ion} of a trapped ion with charge q can be determined by the measurement of its cyclotron frequency in a magnetic field with strength B using [30]

$$\nu_c = \frac{1}{2\pi}\frac{q}{m}B.$$

Following this relation, a calibration of the magnetic field strength needs to be carried out simultaneously with the measurement of the cyclotron frequency of the ion of interest [31]. So far, performing such task is not possible and thus the calibration is done by taking cyclotron frequency measurements of reference ions with a well-known mass before and after the corresponding measurement of the ion of interest. An example of a time-of-flight ion-cyclotron-resonance (TOF-ICR) spectrum can be seen in the inset of figure 1.

Here the stored ions are excited by an azimuthal quadrupole radio-frequency (RF) field and the resonance is detected via the time-of-flight measurement of the ejected ions. The method is destructive, which requires at each RF-frequency step the precision Penning trap to be reloaded with a new bunch of ions. Assuming singly-charged ions, substituting the magnetic field strength (B) with the estimated cyclotron frequency of the reference ion (ν_c^{ref}) and replacing the ion mass ($m_{\mathrm{ion}}^{\mathrm{ref}}$, m_{ion}) of the reference and the ion of interest with the atomic mass (m^{ref}, m) one obtains a relation [32]

$$m = \frac{\nu_c^{\mathrm{ref}}}{\nu_c}\cdot(m^{\mathrm{ref}} - m_e) - m_e,$$

with m_e being the electron mass and ν_c the cyclotron frequency of the ion of interest (omitting the electron binding energy). All frequency ratios $r = \nu_c^{\mathrm{ref}}/\nu_c$ obtained in this work are summarized in table 1.

4. Results

4.1. ^{132}Cs isotope

Three TOF-ICR resonances were obtained. The individual frequency ratios agree to each other within the experimental uncertainties. The resulting mass excess value (as defined on p 1608 of [33]) is ME = −87 151.4(1.2) keV. The new weighted mean frequency ratio corresponds to a result that deviates by about 2σ from the value listed in the Atomic Mass Evaluation 2012 (AME2012) [33].

Table 1. Frequency ratios, mass excesses and half-lives of the measured isotopes of cesium. The mass excess values tabulated in the AME2012 [33] are also given for comparison. The reference mass used in the evaluation is $m(^{133}\mathrm{Cs}) = 132\ 905\ 451.961(9)\ \mu\mathrm{u}$. All ISOLTRAP uncertainties have been computed following the methods described in [34].

A	Half-life	$r = \nu_c^{\mathrm{ref}}/\nu_c$	Mass excess (keV)	
			ISOLTRAP	AME2012
132	6.480(6) d	0.992 483 2589(110)	−87 151.4(1.2)	−87 156.2(2.0)
146	321(2) ms	1.098 078 9375(250)	−55 309(3)	−55 570(40)
147	230(1) ms	1.105 630 4862(673)	−51 920(8)	−52 020(50)
148	146(6) ms	1.113 195 127(1030)	−46 911(13)	−47 300(580)

4.2. ^{146}Cs isotope

The mass excess determined from TOF-ICR measurements is ME = −55 309(3) keV. The literature value in AME2012 is ME = −55 570(40) keV, which deviates from our result by 264 keV. We note that the uncertainty of our new measurement is 3 keV. In the process of data analysis, a second Penning-trap experiment (the CPT situated at the CARIBU facility in Argonne, USA) reported ME = −55 323.2(8.6) keV for the same nuclide. Comparing our new value to the one from the CPT we obtain a difference of 18 keV [35], i.e. a 2σ deviation. Although, the new results slightly disagree, they are by an order of magnitude more precise. Furthermore, they show deviation in the same direction with respect to the mass excess given in AME2012.

4.3. ^{147}Cs isotope

Two previous reports exist for this nuclide, one from 1986 by Orsay's double-focusing mass spectrometer at ISOLDE [21] and one from 2008 by ISOLTRAP [36]. The weighted mean of the mass excesses from both measurements tabulated in AME2012 is ME = −52 020(50) keV. The mass excess derived from our new data is ME = −51 920(8) keV.

4.4. ^{148}Cs isotope

This nuclide was previously investigated only by the Orsay's double-focusing mass spectrometer at ISOLDE [21]. The mass excess reported in that work is ME = −47 300(580) keV. The new and more precise value from the measurements reported here is ME = −46 911(13) keV. We note that although the values agree within the quoted uncertainties our value is by a factor 40 more precise.

5. Discussion

Atomic masses, as determined in this work, and nuclear charge radii, as obtained by optical spectroscopy from isotope shift measurements [30], are two examples of basic properties of nuclei, which are sensitive to the evolution of nuclear structure along an isotopic chain. Indeed, nuclides found at or near shell closures exhibit a spherical ground state, while a smooth or sudden shape evolution occurs by moving towards the mid-shell [37].

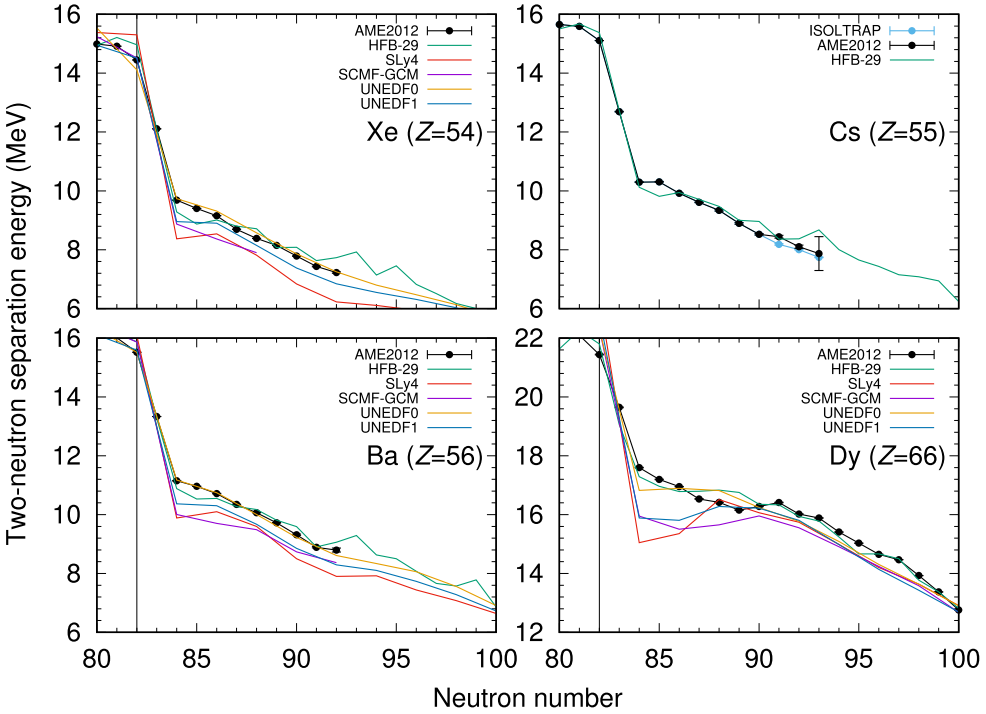

Figure 2. Experimental two-neutron separation energies for xenon (Xe), cesium (Cs) and barium (Ba) and dysprosium (Dy) isotopic chains (black points and lines). The shell-closure at $N = 82$ is indicated by a vertical solid line. The predictions of several mass models are given with colored lines. For details of used models see text.

The connection of these basic properties and nuclear structure becomes evident in the evolution of the two-neutron separation energies (S_{2N}) and the mean-square charge radii. To illustrate the effect of nuclear structure variations with increasing neutron number, the two-neutron separation energies (S_{2N}) and mean-square charge radii are presented in figures 2 and 3 for xenon ($Z = 54$), cesium ($Z = 55$) and barium ($Z = 56$), as well as for the dysprosium ($Z = 66$) isotopic chains. The experimental values have been taken from this work, [33, 38]. In figure 2, the $N = 82$ shell closure becomes apparent as steep drop in the S_{2N} and in figure 3 as a strong change of slope in charge radii. At the same time the onset of deformation in the ground state manifests itself as an increase in the S_{2N} and as an increase of the curvature in the charge radii. A number of nuclei around the neutron-rich ^{146}Cs isotope has been predicted to have octupole deformed equilibrium shapes [39, 40]. For instance, it was found that octupole deformation occurs in ^{144}Xe ($N = 90$), in the isotopes of barium with neutron number $88 < N < 92$ as well as in cerium isotopes with $N = 86$, 88. However, octupole contributions reflected in the separation energies are supposed to be rather small, below 1 or even 0.5 MeV [25, 39]. They are very often hidden by the much stronger quadrupolar deformation, making it even harder to observe an effect in the separation energies. The rare-earth region is a well known example for a prominent quadrupole deformation. One can clearly see the increase in the S_{2N} for the dysprosium isotopic chain at neutron numbers $N > 89$ in figure 2 and the curvature in the charged radii in figure 3.

The atomic masses of the neutron-rich isotopes of cesium determined in this work reveal some interesting information. The results of the measurements smooth out the trend of S_{2N}

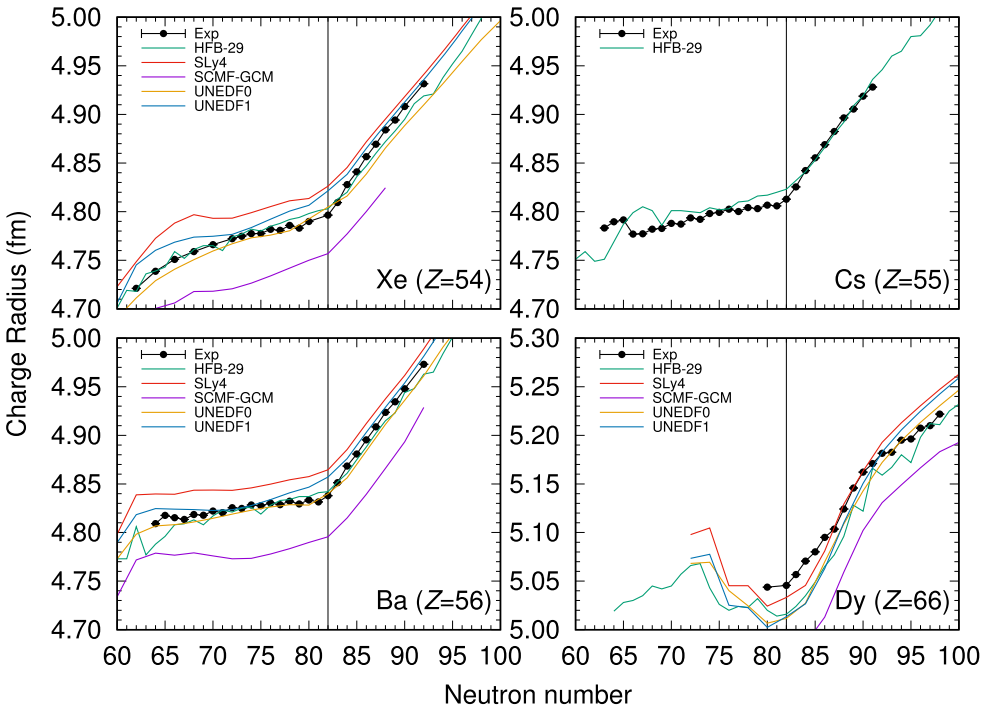

Figure 3. Nuclear charged radii of xenon, cesium and barium isotopic chains obtained from isotope shift measurements as a function of the neutron number. The experimental data were taken from [38].

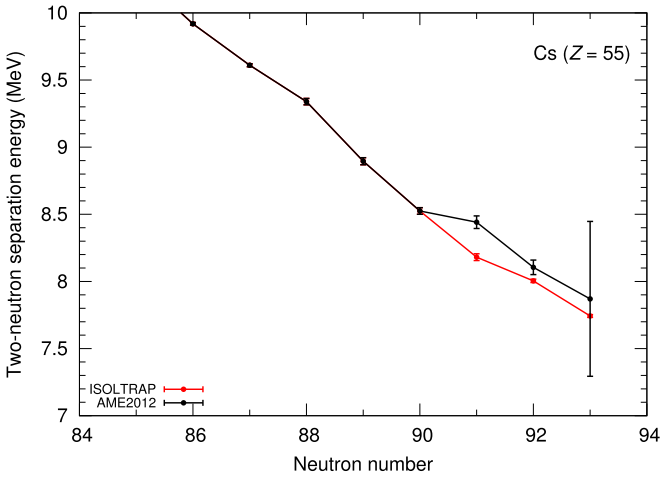

Figure 4. Two-neutron separation energies for the Cs ($Z = 55$) isotopes investigated in this work. For comparison S_{2N} energies derived from AME2012 are also presented. Using the newly obtained data, the trend has been smoothed out removing the kink in the slope at $N = 90$.

values in the cesium isotopic chain and eliminate the kink at $N = 90$ resulting from previous measurements (see figures 2 and 4). With this change, the evolution of the nuclear structure for cesium now seems to resemble closely that of its proton-number neighbors which is in contrast to the heavier chains (such as dysprosium). This smooth evolution is consistent with the general trend of the cesium charge radii (see figure 3). For comparison predictions from several microscopic calculations have been added in figures 2 and 3. Note that with the exception for one mass table, HFB-29, all other selected predictions are only available for even-Z nuclides, i.e. for xenon, barium and dysprosium isotopes.

The selection of microscopic models illustrates the most recent developments in the optimization of self-consistent mean-field approaches using Skyrme-type interactions. The reference is the SLy4 interaction [41], which has been widely employed throughout the years in both the Hartree–Fock–Bogoliubov (HFB) and Bardeen–Cooper–Schrieffer frameworks. The predictions of mean-field calculations performed with this functional are shown with red line. Two other approaches have been employed to further refine the SLy4 model predictions. First, beyond-mean field correlations have been included using the generator-coordinate method (GCM) [42, 43], the results of which are presented with magenta lines. Second, the SLy4 interaction has been used as starting point for advanced optimizations of the nuclear density functional. This lead to the development of the UNEDF0 functional [44] and its subsequent installment, UNEDF1 [45]. The latter has been additionally optimized on other nuclear properties, such as the excitation energies of fission isomers and empirical single-particle energies, respectively. The predictions of the UNEDF functionals are given with orange (UNEDF0) and blue (UNEDF1) lines. All models predict a smooth trend of the S_{2N} in barium and xenon which is in qualitative agreement with experiment. The latter two elements are described by the UNEDF functionals as prolate-deformed systems with a gradual development of quadrupole deformation from $N = 82$ on. In terms of a quantitative agreement, one notices for the SLy4 parametrization that while the relative trends of charge-radii and S_{2N} are well reproduced, they have significant offsets to the experimental values. The GCM formalism improves the description of separation energies, but the charge-radii are significantly underestimated. The best agreement in the barium and xenon isotopic chains is obtained for the UNEDF0 functional. However, one immediately notices that in the case of the dysprosium chain the separation energies are still described only on average. This suggests that the model is missing partly the detailed evolution of the separation energies over the onset of deformation at $N = 90$. Furthermore, it is interesting to point out that the predictions of the UNEDF1 functional, optimized on the same set of masses and charge radii, but including the additional optimization on the fission isomers in ^{240}Pu, gives a slightly worse description of the selected chains in figures 2 and 3. This was also noted by the authors of the UNEDF formalism, referring to the general description of atomic masses and radii. In conclusion, although a large improvement over SLy4 is achieved, the UNEDF0 functional is still not sufficient to describe all nuclear properties with an accuracy adequate for the experimental findings.

The constant development and the exploration of the parameter space by the Brussels–Montreal collaboration is another approach to the complex problem of mass predictions. So far studies have resulted in a global mass table labeled as HFB-29. The mass model has in addition to the generalized Skyrme form a modified spin-orbit force [46]. The force was fitted to essentially all available mass data and at the same time to a realistic equation of state of neutron matter. The mass model predictions are displayed in figures 2 and 3 in green color. By using this particular parametrization, the authors obtained a root-mean-square deviation of 0.52 MeV with respect to the 2353 known masses. In figure 2 one notices fairly good description of the S_{2N} trend for xenon, cesium and barium up to $N = 92$, which is comparable

to the one of the UNEDF0. However, beyond this point the two models significantly disagree in their predictions. Currently, the increase in the S_{2N} predicted by the HFB-29 at $N = 93$ is ruled out by the new mass measurements of ^{148}Cs. Hence, further measurements of cesium, barium and xenon isotopes are necessary in order to establish a definitive departure from the linear trend at higher neutron number.

6. Summary

Throughout the last three decades, the ISOLTRAP collaboration has performed mass measurements on short-lived nuclei with relative mass uncertainties as low as 10^{-8}. In this work we reported the atomic masses of several neutron-rich cesium nuclides. Our investigations of the two-neutron separation energies clear out an apparent kink from previous measurements interpreted as an onset of deformation. The new results suggest that there are no major structural changes up to ^{148}Cs. The mass differences exhibit a monotonous decrease toward the neutron drip-line, a behavior also present in the neighboring isotopic chains of xenon and barium. We have compared our experimental data to the predictions of several microscopic models. The selected models describe well the observed smooth behavior of the S_{2N} values, although the predictive power of the models is still about 2 orders of magnitude lower than the uncertainties of the presented mass measurements. A quantitative agreement was found with the UNEDF0 and HFB-29 functionals up to neutron number $N = 92$. The new mass of ^{148}Cs rules out any sudden increase in nuclear collectivity of the cesium isotopes at $N = 93$.

Acknowledgments

This work was supported by the BMBF under Contracts No. 05P12HGCI1, No. 05P12HGFNE, and No. 05P09ODCIA, the EU through ENSAR (Grant No. 262010), the French IN2P3, the ISOLDE Collaboration, by the Helmholtz Association (HGF) through the Nuclear Astrophysics Virtual Institute, the IMPRS-PTFS, and the Max-Planck Society. SK acknowledges support from the Robert-Bosch Foundation, RBC from the Max-Planck Partner Group with MPIK and by the Istanbul University Scientific Research Projects, Number 26435. TE from the Alexander von Humboldt foundation. YuAL acknowledges the Helmholtz-CAS Joint Research Group HCJRG-108. We would like to thank the ISOLDE target team for producing the cesium beam despite exceptional technical difficulties and the ISOLDE operations team for their support.

References

[1] Kugler E 2000 *Hyperfine Interact.* **129** 23–42
[2] Atanasov D *et al* 2015 *Phys. Rev. Lett.* **115** 232501
[3] Rosenbusch M *et al* 2015 *Phys. Rev. Lett.* **114** 202501
[4] Böhm Ch *et al* 2014 *Phys. Rev.* C **90** 044307
[5] Manea V *et al* 2013 *Phys. Rev.* C **88** 054322
[6] Wienholtz F *et al* 2013 *Nature* **498** 346–9
[7] Wolf R N *et al* 2013 *Phys. Rev. Lett.* **110** 041101
[8] Epherre M *et al* 1979 *Phys. Rev.* C **19** 1504–22
[9] Audi G *et al* 1982 *Nuc. Phys.* A **378** 443–60
[10] Kluge H-J 2013 *Int. J. Mass Spectrom.* **349–350** 26–37
[11] Kluge H-J 1988 *Phys. Scr.* **T22** 85
[12] Eronen T, Kankainen A and Äystö J 2016 *Prog. Part. Nucl. Phys.* **91** 259–93

[13] Blaum K 2006 *Phys. Rep.* **425** 1–78
[14] Lunney D, Pearson J M and Thibault C 2003 *Rev. Mod. Phys.* **75** 1021–82
[15] Mumpower M *et al* 2015 *J. Phys.* G **42** 034027
[16] Arcones A and Martínez-Pinedo G 2011 *Phys. Rev.* C **83** 045809
[17] Schatz H *et al* 1998 *Phys. Rep.* **294** 167–263
[18] Stolzenberg H *et al* 1990 *Phys. Rev. Lett.* **65** 3104–7
[19] Bollen G 1993 *Hyperfine Interact.* **78** 57–66
[20] Blaum K *et al* 2002 *Proc. 3rd Int. Conf. on 'Fission and Properties of Neutron-Rich Nuclei' FPNRN* (New Jersey: World Scientific) pp 655–62
[21] Audi G *et al* 1986 *Nucl. Phys.* A **449** 491–518
[22] Herfurth F *et al* 2001 *Nucl. Instrum. Methods* A **469** 254–75
[23] Wolf R N *et al* 2012 *Nucl. Instrum. Methods* A **686** 82–90
[24] Wolf R N *et al* 2013 *Int. J. Mass Spectrom.* **349–350** 123–33
[25] Mukherjee M *et al* 2008 *Eur. Phys. J.* A **35** 1–29
[26] Kreim S *et al* 2013 *Nucl. Instrum. Methods* B **317** 492–500
[27] Wolf R N, Marx G, Rosenbusch M and Schweikhard L 2012 *Int. J. Mass Spectrom.* **313** 8–14
[28] Bradbury N E and Nielsen R A 1936 *Phys. Rev.* **49** 388–93
[29] Savard G *et al* 1991 *Phys. Lett.* A **158** 247–52
[30] Blaum K, Dilling J and Nörtershäuser W 2013 *Phys. Scr.* **T152** 014017
[31] Blaum K *et al* 2003 *J. Phys.* B **36** 921
[32] König M *et al* 1995 *Int. J. Mass Spectrom.* **142** 95–116
[33] Audi G *et al* 2012 *Chin. Phys.* C **36** 1287
[34] Kellerbauer A 2003 *Int. J. Mass Spectrom.* **229** 107–15
[35] Van Schelt J *et al* 2013 *Phys. Rev. Lett.* **111** 061102
[36] Weber C *et al* 2008 *Nuc. Phys.* A **803** 1–29
[37] Shimizu N *et al* 2001 *Phys. Rev. Lett.* **86** 1171–4
[38] Angeli I and Marinova K P 2013 *At. Data Nucl. Data Tables* **99** 69–95
[39] Nazarewicz W *et al* 1984 *Nucl. Phys.* A **429** 269–95
[40] Neidherr D *et al* 2009 *Phys. Rev.* C **80** 044323
[41] Chabanat E *et al* 1998 *Nucl. Phys.* A **635** 231–56
[42] Bender M, Heenen P-H and Reinhard P-G 2003 *Rev. Mod. Phys.* **75** 121–80
[43] Bender M, Bertsch G F and Heenen P-H 2006 *Phys. Rev.* C **73** 034322
[44] Kortelainen M *et al* 2010 *Phys. Rev.* C **82** 024313
[45] Kortelainen M *et al* 2012 *Phys. Rev.* C **85** 024304
[46] Goriely S 2015 *Nuc. Phys.* A **933** 68–81